Journal of Biomedical Optics

SPIEDigitalLibrary.org/jbo

Hemoglobin parameters from diffuse reflectance data

Judith R. Mourant
Oana C. Marina
Tiffany M. Hebert
Gurpreet Kaur
Harriet O. Smith

SPIE

Hemoglobin parameters from diffuse reflectance data

Judith R. Mourant,[a,*] Oana C. Marina,[a] Tiffany M. Hebert,[b] Gurpreet Kaur,[c] and Harriet O. Smith[c]
[a]Bioscience Division, Los Alamos National Laboratory, Los Alamos, P.O. Box 1663, MS M888, New Mexico 87544
[b]Jack D. Weiler Hospital, 1825 Eastchester Road, Room 3-37, Bronx, New York 10461
[c]Einstein Cancer Center, Department of Obstetrics and Gynecology and Women's Health, 1695 Eastchester Road, Bronx, New York 10461

Abstract. Tissue vasculature is altered when cancer develops. Consequently, noninvasive methods of monitoring blood vessel size, density, and oxygenation would be valuable. Simple spectroscopy employing fiber optic probes to measure backscattering can potentially determine hemoglobin parameters. However, heterogeneity of blood distribution, the dependence of the tissue-volume-sampled on scattering and absorption, and the potential compression of tissue all hinder the accurate determination of hemoglobin parameters. We address each of these issues. A simple derivation of a correction factor for the absorption coefficient, μ_a, is presented. This correction factor depends not only on the vessel size, as others have shown, but also on the density of blood vessels. Monte Carlo simulations were used to determine the dependence of an effective pathlength of light through tissue which is parameterized as a ninth-order polynomial function of μ_a. The hemoglobin bands of backscattering spectra of cervical tissue are fit using these expressions to obtain effective blood vessel size and density, tissue hemoglobin concentration, and oxygenation. Hemoglobin concentration and vessel density were found to depend on the pressure applied during *in vivo* acquisition of the spectra. It is also shown that determined vessel size depends on the blood hemoglobin concentration used. [DOI: 10.1117/1.JBO.19.3.037004]

Keywords: cancer detection; hematocrit; hemoglobin concentration; vessel diameter; cervical intraepithelial neoplasia.

Paper 130884R received Dec. 17, 2013; revised manuscript received Feb. 11, 2014; accepted for publication Feb. 18, 2014; published online Mar. 26, 2014.

1 Introduction

Blood vessel density and size are important clinical parameters for the diagnosis of cancerous and precancerous conditions. Microvessel density has been shown to increase in several premalignant conditions.[1] Vascular changes occur quite early in the disease progression leading to colon cancer based on a study of a well-established model system.[2] In oral tissue, microvessel density is reported to increase as pathology changes from normal to dysplastic to squamous cell carcinoma.[3,4] For breast cancer, some studies have demonstrated a correlation between angiogenesis (microvessel density) and clinicopathologic parameters, although there are discrepancies in results, some of which likely arise as a consequence of the variety of techniques (e.g., immunohistochemistry and visual microscopy) used to assess angiogenesis and microvessel density.[5] Neovascularization plays an important role in cervical intraepithelial neoplasia (CIN) as summarized by Chang et al.[6] Microvessel density increases with severity of CIN as assessed by counting of blood vessels in biopsy specimens.[7–9] The results of Dobbs et al.[7] and Obermair et al.[9] are summarized in Table 1. Both the studies demonstrated that microvessel density increases with CIN, but there are discrepancies in the absolute numbers demonstrating that even the counting of blood vessels in biopsy samples is not standardized.

Angiogenesis can be assessed *in vivo* by optical measurements. Hemoglobin concentration and/or oxygenation are frequently derived parameters in optical diagnostic measurements. For example, optically determined higher hemoglobin concentrations in breast tissue are associated with cancer.[10] However, the ability to obtain accurate values of these parameters from light transport measurements is frequently hindered by several factors: hemoglobin is not distributed homogeneously, the pathlength through tissue is not known, and the tissue may be compressed by the measurement probe.

The effects of the nonhomogeneous distribution of hemoglobin on the extraction of the absorption coefficient, μ_a, have been previously studied. Correction factors for a bulk tissue absorption coefficient, μ_a, have been derived by several groups[11–14] and are shown to be similar by van Veen et al.[15] All of these correction factors depend only on the blood vessel radius and the absorption coefficient of blood, but not the density of blood vessels. Here, we present a simple derivation for a correction factor for μ_a due to blood being heterogenously distributed and demonstrate that the correction factor also depends on the density of blood vessels. Our results are compared to the correction factor of Svaasand et al.[11] which is the most commonly used expression due to its simplicity.

This new expression for the effective absorption coefficient is used in a data fitting procedure to extract blood vessel size and density from *in vivo* measurements of cervical tissue. The measurements were made in a backscattering geometry; therefore, the fitting procedure must take into account decreases in pathlength that occur with increasing absorption. We quantitate this effect using Monte Carlo simulations.

Many previous implementations of correction factors for μ_a have assumed a blood hemoglobin concentration of 15 g/dL.[16–19] For most of our patients, clinical blood hematocrit and hemoglobin concentrations were available and consequently, we were able to examine the effect of blood hemoglobin

*Address all correspondence to: Judith R. Mourant, E-mail: jmourant@lanl.gov

Table 1 Microvessel density: number of vessels in a 0.25 mm^2 area of tissue.

	Dobbs et al.[7]	Obermair et al.[9]
Normal	27	
CIN 1	36	19.4 ± 5.8
CIN 2	39	21.9 ± 7.0
CIN 3	46	34.1 ± 14.8
Invasive SCC	54	

concentration on the extracted hemoglobin and vasculature parameters.

Finally, we demonstrate that the force used to hold the optical probe onto the tissue can result in an artificial decrease in the measured hemoglobin concentration and vessel density. Our results are compared with those in the published literature.

2 Obtaining in vivo Data

Data were obtained using a modified 3-mm diameter fiber optic probe described previously.[20] The light delivery and collection fibers are 200 μm in diameter and the delivery fiber is angled 20 deg from normal. The probe was modified to incorporate a pressure sensor as shown schematically in Fig. 1. The 50 μm diameter optical pressure sensor was packaged into a 1-mm diameter cable and sealed with silicone (FISO Technologies, Quebec, Canada). The measurements were performed by gently placing the probe in contact with the tissue, taking a measurement, then adjusting the measurement time for better signal-to-noise. A second measurement was then taken followed by a measurement with the excitation light off to determine the contribution of background light. The light illumination time was <1 s for each measurement. The background light was significant because all measurements were made with the colposcope illumination on. All background subtracted spectra were divided by a reference spectrum that was obtained after each patient was measured. The reference measurement was acquired by putting the probe in gentle contact with Spectralon (Labsphere Inc., North Sutton, New Hampshire) in water. Immersing Spectralon in water induces a small monotonically decreasing wavelength dependence to the measured intensity. This wavelength dependence is accounted for in our analysis. [It will alter the value of the fit parameter c_4 in Eq. (10).] The *in vivo* measurements were completed within 30 s of the probe being placed on the tissue.

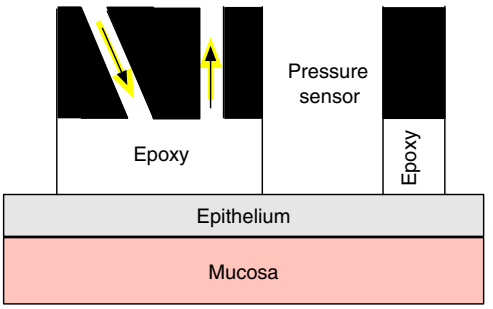

Fig. 1 The geometry used for the measurements. The fiber optics were 200 μm in diameter with a numerical aperture of 0.37 and were embedded in black carbon. The epoxy spacer was several hundreds of microns thick.

In vivo spectra were obtained from patients regularly scheduled for colposcopy at Montefiore Hospital at Albert Einstein Medical Center. Informed consent was obtained for all 14 patients whose data are presented in this study. Two to four sites were measured for each patient after the addition of 3% acetic acid. All sites were measured once and then the measurements were repeated. All measurements were performed by the same doctor and the applied force was recorded for each measurement. After completion of the measurements, biopsies were obtained and individually labeled for later correlation of the histopathology with spectroscopic measurements.

Standard hospital histopathology was performed for each biopsy as well as a separate histopathology analysis by a study pathologist. Hemoglobin concentrations determined from venous blood draws were obtained from hospital records when the measurements had occurred in the previous 6 months. Data were available for all but two patients.

3 Derivation of Equations for Fitting in vivo Data to Determine Absorption

3.1 *Inhomogeneous Absorption*

The size of a blood vessel and its orientation with regards to the incident light direction are important factors in determining the amount of light absorbed by hemoglobin. For illustrative calculations, we consider a straight blood vessel of radius r in a cubical tissue compartment of length L. The two cases of the blood vessel oriented along the axis of light travel and oriented perpendicular to light travel are shown schematically in Figs. 2(a) and 2(b), respectively.

When light impinges on the cubical volume shown in Fig. 2(a), the transmitted light is a sum of the light that did not impinge on the vessel and the light that passed through the blood vessel without being absorbed. The expression for the transmitted light is given by

$$I_{\text{vessel-end-on}} = I_o \left[\frac{L^2 - \pi r^2}{L^2} + \frac{\pi r^2}{L^2} e^{-\epsilon(\lambda) C_b L} \right], \tag{1}$$

where I_o is the incident light intensity, $\epsilon(\lambda)$ is the wavelength dependent molar extinction coefficient of hemoglobin, and C_b is the concentration of hemoglobin in blood.

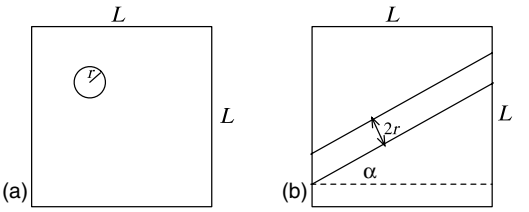

Fig. 2 Schematic of the geometry used for the derivation of a correction factor for μ_a. Light is assumed to be incident perpendicular to the page. r is the radius of the blood vessel and L is the length of the side of a cube of tissue. (a) Schematic of a blood vessel parallel to the direction of light travel. (b) Schematic for a blood vessel perpendicular to the direction of light travel.

The effective absorption coefficient is then

$$\mu_{\mathrm{a,eff,end\text{-}on}} = \left(-\ln\left[\frac{L^2-\pi r^2}{L^2}+\frac{\pi r^2}{L^2}e^{-\epsilon(\lambda)C_{\mathrm{b}}L}\right]\right)/L. \quad (2)$$

If the same amount of blood was distributed homogeneously, then

$$I = I_{\mathrm{o}}e^{-\epsilon(\lambda)C_{\mathrm{b}}(\pi r^2/L^2)L} \quad \text{and} \quad \mu_{\mathrm{a,end\text{-}on}} = \epsilon(\lambda)C_{\mathrm{b}}(\pi r^2/L^2). \quad (3)$$

Values of L and r can be approximated from measurements reported in the literature.[7] The measured mean diameter ranged from 13.99 μm for normal tissue to 15.30 μm for invasive squamous cell carcinoma.[7] For illustrative purposes, we use $r = 7.25$ μm. The initial value used for mean vessel density is taken from the same reference, and we use the value for CIN I which is 36 (Table 1) in a 0.25 mm^2 (0.5 mm)^2 area. This is the same as one vessel per $(0.5/6\,\mathrm{mm})^2 = (0.083\,\mathrm{mm})^2$ area. Therefore, we use $L = 83$ μm in initial calculations.

The wavelength dependent correction to the homogeneous absorption coefficient due to the blood being inhomogeneously distributed as in Fig. 2(a) is shown by the black line in Fig. 3(a). The blood is assumed to be completely oxygenated, the hemoglobin blood concentration, C_{b}, is 0.0054 M (150 mg/ml), and $\epsilon_{\mathrm{oxy}}(\lambda)$ is taken from Ref. 21. The effective absorption coefficient for heterogeneously distributed blood is seen to be much less than for homogeneously distributed blood when the absorption is large.

If the blood vessel cuts across the tissue cube as in Fig. 2(b), then the transmitted light can be approximated as

$$I_{\mathrm{vessel\text{-}across}} = I_{\mathrm{o}}\left[\frac{L^2-sL/\cos(\alpha)}{L^2}+\frac{sL/\cos(\alpha)}{L^2}e^{-\epsilon(\lambda)C_{\mathrm{b}}s}\right], \quad (4)$$

where $s^2 = \pi r^2$. Consequently,

$$\mu_{\mathrm{a,eff,across}} = \left(-\ln\left[\frac{L^2-sL/\cos(\alpha)}{L^2}+\frac{sL/\cos(\alpha)}{L^2}e^{-\epsilon(\lambda)C_{\mathrm{b}}s}\right]\right)/L. \quad (5)$$

For the corresponding case of homogeneous absorption

$$I = I_{\mathrm{o}}e^{-\epsilon(\lambda)C_{\mathrm{b}}\left(s^2\frac{L}{\cos(\alpha)}/L^3\right)L} \quad \text{and} \quad \text{for } \alpha = 0$$
$$\mu_{\mathrm{a,across}} = \epsilon(\lambda)C_{\mathrm{b}}(\pi r^2/L^2). \quad (6)$$

The fractional decrease in absorption due to the blood being distributed heterogeneously as in Fig. 2(b) is plotted as a function of wavelength for oxygenated hemoglobin in Fig. 3(a) as colored lines with markers. There is very little effect due to α being nonzero. Therefore, α will be assumed to be zero for the rest of this work.

Figure 3(a) demonstrates that the effect of constraining the blood to be within the vessels is much greater when the vessels are parallel to the incident light. For the (parallel) end-on case, most of the light does not "see" any of the absorber when $L \gg r$, as is evident from Eq. (1). Also, while the absorption coefficient is greater by a factor of $L^2/\pi r^2$, the absorption of this small fraction of the incident light is much less than the absorption

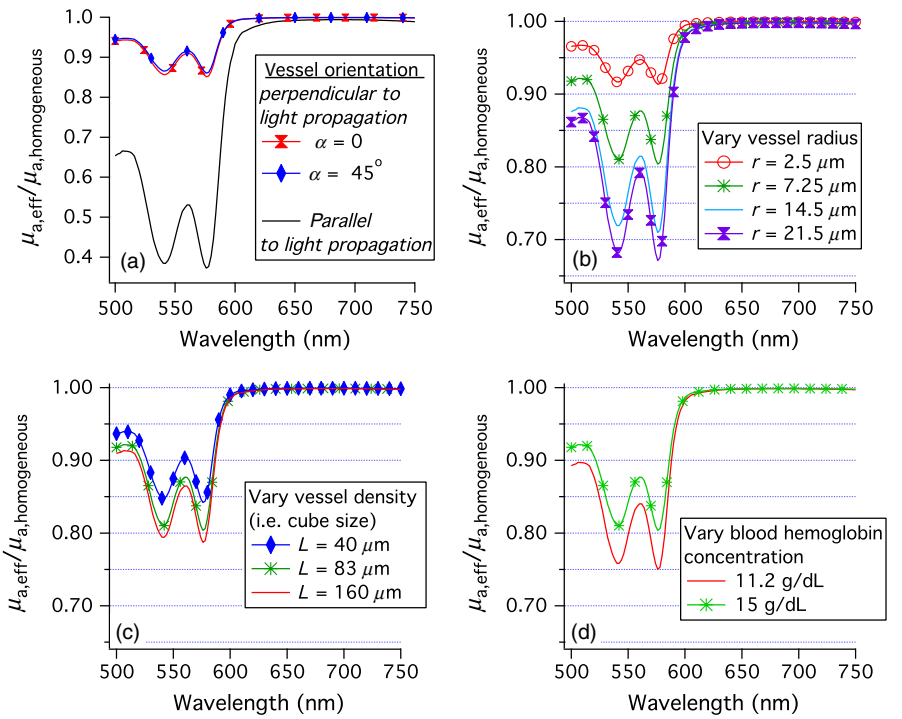

Fig. 3 Ratios of the effective optical absorption coefficient for oxygenated blood in a vessel to the absorption coefficient if the blood were distributed homogeneously. (a) The black line correponds to the vessel orientation of Fig. 2(a) and the colored (lighter) lines correspond to the vessel orientation of Fig. 2(b). (b–d) The average ratio of the effective absorption coefficient for oxygenated blood in a vessel to the absorption coefficient if the blood was distributed homogeneously. Unless otherwise stated in the captions, $L = 83$ μm, $r = 7.25$ μm, and the hemoglobin concentration of blood was 15 g/dL.

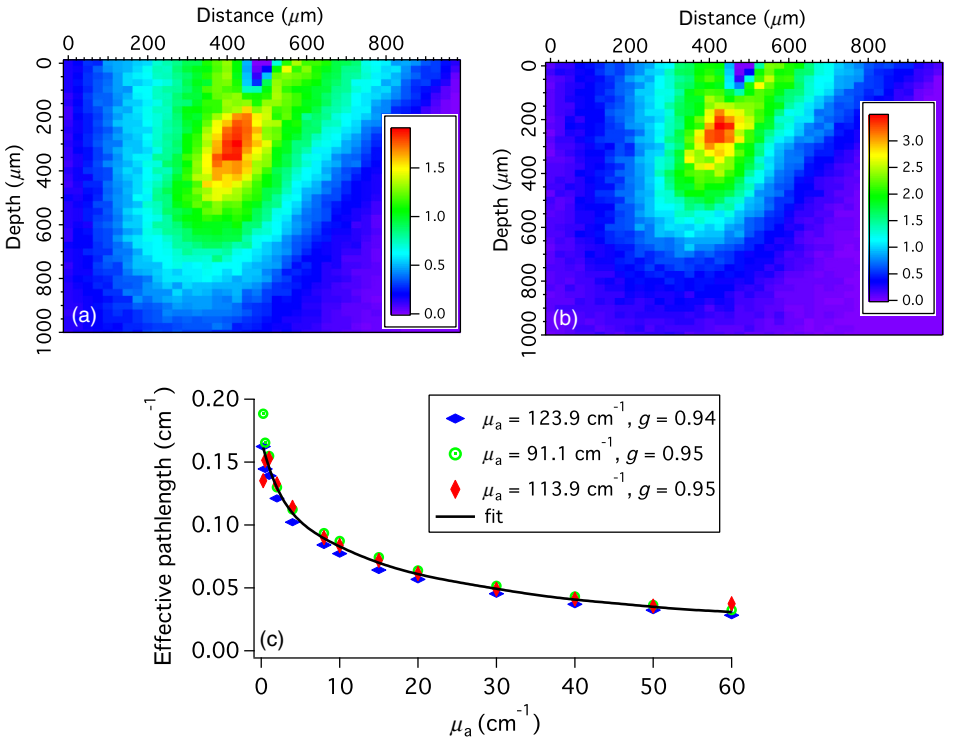

Fig. 4 (a and b) The density of scattering events (summed over the axis perpendicular to the page). For (a) $\mu_a = 0$ and for (b) $\mu_a = 10$ cm^{-1}. The color scale is the number of scattering events per pixel. (c) The effective pathlength over which absorption occurs. The data points were calculated via Eq. (7) using Monte Carlo simulations. Each type of symbol represents a different set of scattering parameters. The black line is a polynomial fit to all of the data.

when the blood is distributed homogeneously. For the perpendicular or "across" case, a much greater fraction of the incident light sees the absorber.

If vessels are assumed to be oriented randomly with regards to the direction of light travel, an effective correction factor for the effects of the blood being contained in blood vessels on the measurement of absorption can be determined by averaging over the possible orientations of the blood vessel with regards to the incident light. The assumption of random angles between vessels and light propagation is based on the morphology of tissue and knowledge of how light propagates. For normal stroma, most vessels are roughly parallel to the surface of the tissue. However, for high grade CIN blood vessels can branch up into the epithelium sometimes becoming nearly perpendicular to the tissue surface.[22] The direction of light travel varies with depth. It is roughly perpendicular to the tissue surface in the top of the cellular epithelium, but can be parallel to the tissue surface in the stroma. Due to the variations in light propagation and vessel orientation, we assume that the orientation of light propagation with regards to vessel orientation is random.

The averaging over relative orientations of the vessels and light propagation direction is performed in spherical coordinates with the z-axis being into the page in Fig. 2. Using the physics convention, θ is the polar angle, while ϕ is the azimuthal angle. We assume that ϕ does not affect the absorption of light. Figures 3(b)–3(d) show correction factors for a number of conditions and are discussed in Sec. 4.

3.2 *Change in Pathlength Due to Absorption*

In transmission geometries such as those shown in Fig. 2, the pathlength does not depend on absorption. However, in the backscattering geometry typically used for interrogating tissue, the average pathlength traveled by photons will depend on $\mu_a(\lambda)$. To illustrate this phenomenon, Monte Carlo simulations of light propagation in the cervical epithelium were performed. The top 300 to 400 μm of normal cervical epithelium is cellular with no penetration of blood vessels. Consequently, in the simulations no absorption is allowed in the top 300 μm. The density of scattering events summed over the axis perpendicular to the page are shown in Fig. 4, for $\mu_a = 0$ and $\mu_a = 10$ cm^{-1}. The scattering parameters were $\mu_s = 91.1$ cm^{-1}, $g = 0.95$, yielding $\mu_s' = 4.2$ cm^{-1}. In the case of higher absorption, the relative density of scattering events is greatly reduced at depths >300 μm. Furthermore, trajectories that start or end near the edges of the fibers, which will on an average be longer, are less likely when the absorption is greater.

Simulations were run in which μ_a varied from 0 to 60 cm^{-1} for three sets of scattering parameters: $\mu_s = 113.9$ cm^{-1}, $g = 0.95$, yielding $\mu_s' = 5.3$ cm^{-1}; $\mu_s = 91.1$ cm^{-1}, $g = 0.95$, yielding $\mu_s' = 4.2$ cm^{-1}; and $\mu_s = 123.9$ cm^{-1}, $g = 0.94$, yielding $\mu_s' = 7.5$ cm^{-1}. For each simulation, an effective absorption pathlength, p_{eff}, was calculated as

$$p_{\text{eff}}(\mu_a) = \ln\left(\frac{I(\mu_a)}{I(0)}\right)/\mu_a, \tag{7}$$

where I is the intensity of the collected light (i.e., the number of collected photons). The effective pathlengths are shown in Fig. 4(c) with a different symbol for the three sets of scattering parameters. For each value of μ_a, the results for different scattering parameters were averaged and the resulting data were fit to a ninth-order polynomial. The result is the thick black line in

Fig. 4(c). These results would change if the tissue or measurement geometry changed.

3.3 *Fitting the Spectra*

Measured *in vivo* spectra were fit to

$$I = I(0)e^{-\mu_{a,\mathrm{eff}} p_{\mathrm{eff}}(\mu_{a,\mathrm{eff}})}, \tag{8}$$

where $\mu_{a,\mathrm{eff}}$ is the effective absorption coefficient and p_{eff} was determined and parameterized as described above.

To vary the size of the blood vessels, we use $r = c_0 \times 7.25\ \mu$m and $s = \sqrt{(\pi r^2)}$, where c_0 is a fit parameter. c_0 is constrained so that the smallest vessel diameter is 4 μm, which is a good estimate of the smallest diameter capillary in humans.[23] To vary the density of blood vessels, we use $L = c_5 \times 83\ \mu$m, where c_5 is a fit parameter.

The extinction coefficient for blood, $\epsilon(\lambda)$, is given by Eq. (9), where the fit parameter c_1 is hemoglobin oxygenation

$$\epsilon(\lambda) = (1 - c_1)\epsilon_{\mathrm{Hb}}(\lambda) + c_1\epsilon_{\mathrm{HbO_2}}(\lambda). \tag{9}$$

The light intensity $I(0)$ in Eq. (8) is not the light incident on the tissue, rather it is the emitted light intensity from tissue in the case of no absorption. It can be estimated from portions of the spectra that do not have any absorption. We assume it has the functional form of

$$I(0) = c_2 + c_3\lambda^{c_4}, \tag{10}$$

where c_2, c_3, and c_4 are the fit parameters.

The data were fit over the wavelength range of 520 to 732 nm. Example fits are shown in Fig. 5.

4 Results

4.1 *Dependence on Vessel Density, Size, and Blood Hemoglobin*

The correction factor depends on several features, vessel density, vessel radius, and hemoglobin blood concentration. The dependence on vessel radius is well known; Fig. 3(b) shows that as the vessel radius is increased, the value of the correction factor decreases. The dependence of the correction factor on vessel density has not been accounted for previously. Figure 3(c) shows that as vessel density increases, the correction factor becomes closer to 1. Finally, we show that the correction factor depends on the concentration of hemoglobin in the blood vessels in Fig. 3(d). As the concentration of hemoglobin in the blood increases, the correction factor becomes closer to 1.

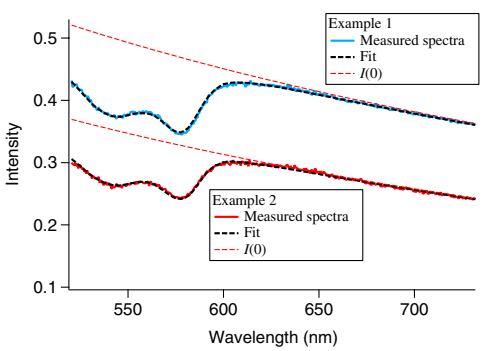

Fig. 5 Examples of *in vivo* measurements and fits to the model of this paper.

4.2 *Comparison to Previously Published Correction Factors*

The data were fit using both the correction factor originally derived by Svaasand[11] and stated concisely by van Veen et al.,[15] as well to our correction factor. The Svaasand correction factor is given by Eq. (11). In Eq. (11), $\epsilon(\lambda)$ is as defined previously in Eq. (9), and r is the vessel radius. Both methods have the same number of fit parameters, six. Several of them are the same: c_0 is the relative vessel size, c_1 is the oxygenation, c_2, c_3, and c_4 are used in the parameterization of the measured backscattering signal in the absence of absorption [Eq. (10)]. The fit parameter, c_5, however, is different. When the Svaasand correction factor is used, it is the blood volume fraction as in Eq. (12). When our correction factor is used, c_5 controls the density of blood vessels through the equation $L = c_5 \times 83\ \mu$m and the tissue $\mu_{a,\mathrm{eff}}$ is given by Eq. (13)

$$C_{Sv} = \frac{\mu_{a,\mathrm{eff}}}{\mu_a} = \frac{1 - e^{-2\epsilon(\lambda)C_b r}}{2\epsilon(\lambda)C_b r}, \tag{11}$$

$$\mu_{a,\mathrm{eff}} = c_5\epsilon(\lambda)C_{Sv}, \tag{12}$$

$$\mu_{a,\mathrm{eff}} = \frac{\pi r^2}{L^2}C_b\epsilon(\lambda)C_{\mathrm{this\ work}} \tag{13}$$

Figure 6 compares the tissue hemoglobin concentration, average vessel radius, and oxygenation obtained with our correction factor and with the correction factor of Svaasand. Higher tissue hemoglobin concentrations are found with the Svaasand method except at the highest concentrations where the trend is toward more similar concentrations. The average change was 150% ± 120%. For all parameters, the results are well correlated, although there are some clear discrepancies. Most changes in oxygenation were in the −20% to +20% range. Vessel size

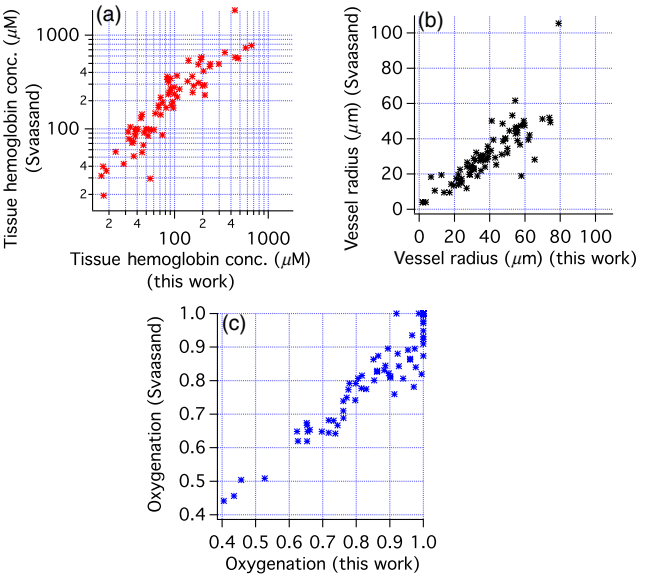

Fig. 6 Comparison of results of fitting *in vivo* spectra using either the correction factor derived in this paper or by Svaasand as written by van Veen. (a) Tissue hemoglobin concentration, (b) vessel radius, and (c) oxygenation.

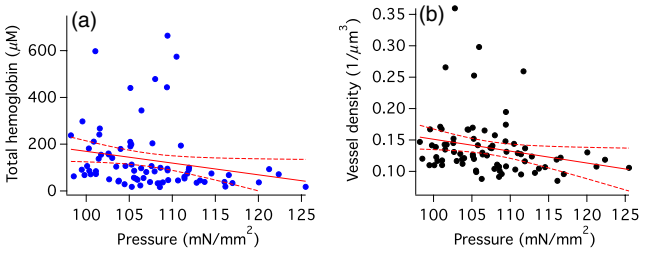

Fig. 7 (a) Hemoglobin concentration versus probe pressure for 80 measurements. (b) Vessel density versus the pressure. Straight line fits and confidence intervals are shown.

was slightly smaller with the Svaasand correction factor, with changes ranging from 0% to 50%.

4.3 *Effects of Force on Measured Hemoglobin Concentration*

For each measurement, the force used to hold the probe against the tissue was measured and recorded. The amount of hemoglobin present decreases with the force used as shown in Fig. 7(a). To quantify this result, we tested the hypothesis that the average hemoglobin concentration measured with a pressure <112 mN/mm^2 was greater than the average hemoglobin concentration measured with a pressure >112 mN/mm^2. A T-test shows that the hypothosis is correct ($\alpha = 0.01$). Additionally, a straight line was fit to the data and found to have a negative slope at the 93% confidence level. Vessel density appears to decrease with probe pressure as shown in Fig. 7(b). The slope was <1 at the 95% confidence level. Vessel size and hemoglobin oxygenation, however, did not show a dependence on the force used to hold the probe against the tissue.

4.4 *Relationship of Pathology to Hemoglobin Parameters*

The study pathologist categorized each biopsy as normal, cervicitis, metaplasia, LSIL (CIN 1), or HSIL (CIN 2/3). These categories were then coalesced into three categories normal (includes normal, cervicitis, and metaplasia), CIN 1, and CIN 2/3. The CIN 1 and CIN 2/3 classifications were also used in the hospital pathology reports. All other biopsies were initially classified as normal. Table 2 compares the hospital pathology with the study pathologist's results. The top line shows that 4 of the 25 sites classified as normal by hospital pathology were classified as CIN 1 by the study pathologist. The first column shows that of the 24 sites classified as normal by the study pathologist, 3 of those were classified as CIN 1 in hospital pathology. This table also demonstrates discrepancies in the classification of biopsy samples as CIN 1 or CIN 2/3.

Table 2 Study pathologist results versus hospital pathology results.

	Normal	CIN 1	CIN 2/3	Totals for hospital pathology
Normal by hospital pathology	21	4	0	25
CIN 1 by hospital pathology	3	2	0	5
CIN 2/3 by hospital pathology	0	2	1	3
Totals for study pathologist	24	8	1	

To assess trends between the measured hemoglobin parameters and pathology, the worst pathology diagnosis for each site was used, which resulted in 21 normal sites, 9 CIN 1 sites, and 3 CIN 2/3 sites. For most sites, two spectroscopy measurements were averaged and the average of those measurements are shown as large symbols in Fig. 8. Sites with single measurements have small symbols. Vessel density versus hemoglobin oxygenation are plotted in Fig. 8(a) and vessel radius versus tissue hemoglobin concentration are shown in Fig. 8(b). The CIN 2/3 site for which there was agreement in the histopathology is a solid brown square with a circle around it. The two sites for which the hospital pathology report result was CIN 2/3 are orange bow ties. On both the graphs, the brown square appears on the edge of where the majority of the data are plotted. Another trend is that the CIN 1 sites tended to have low total hemoglobin and low vessel density.

The normal sites had a wide range of parameter values. To assess whether any of the subsets of the normal sites correlated with hemoglobin, the normal sites were coded as inflammed, metaplastic, cervicitis, or just plain normal. None of these subsets correlated with any of the hemoglobin parameters. The study pathologist determined that all of the biopsies were from either the squamous–columnar junction or of ectocervix (squamous epithelium). Neither tissue type was confined to any region of the graphs in Fig. 8. However, all of the sites with both a low tissue hemoglobin content <50 μM and a vessel radius <36 μm were squamous epithelium only.

4.5 *Correlations Between Hemoglobin Parameters*

A small-to-medium vessel radius and high tissue hemoglobin concentration are rare in Fig. 8(b). To determine where those sites are on the plot of vessel density versus oxygenation, some of the sites are labeled with numbers in all of the panels in Fig. 8. Those few sites that have a small vessel radius and high hemoglobin concentration have a high vessel density as shown in Fig. 8(a).

A plot of oxygenation versus tissue hemoglobin concentration [Fig. 8(c)] shows a line of points along the top with saturated oxygenation and a large variation in tissue hemoglobin concentration. The rest of the data shows a trend of decreasing oxygenation with increasing tissue hemoglobin.

4.6 *Effect of Using Venous Hemoglobin Concentrations*

Data from 12 patients were refit using available patient specific venous hemoglobin concentrations. There were no venous hemoglobin concentrations available for the other two patients, so the average value of 12.9 g/dL was used. Oxygenation changed by <2% for all but two sites. Vessel density showed small changes, with only one site changing by >10%. Vessel radius was greater for all but two sites. The increase was $19 \pm 12\%$. Tissue hemoglobin changed by <5% for most sites, but for 13 sites there were more significant changes with some being increases and others being decreases. The changes were quite large in some cases. Figure 8(d) shows vessel radius versus tissue hemoglobin concentration results when

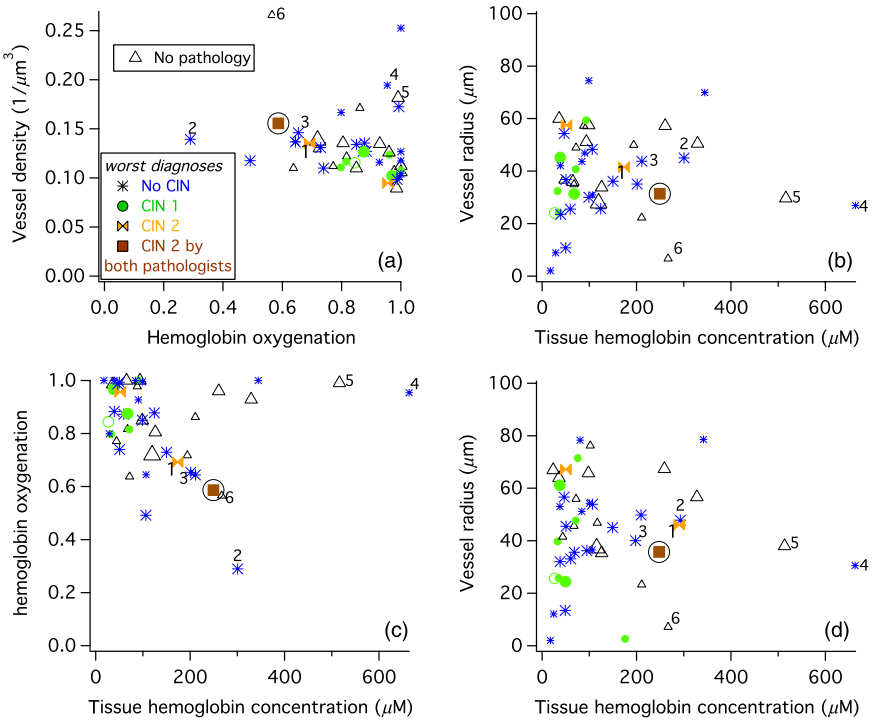

Fig. 8 Results for 49 sites. Large symbols are averages of two (or three) spectroscopic measurements. The pathology is denoted by a color and marker as denoted in the legend of panel (a). Some sites are numbered so that their location can be compared in different panels. (a–c) Results of fits performed assuming a blood hemoglobin concentration of 15 g/dL. (d) Results of fits performed using venous blood hemoglobin measurements.

the data are fit with patient specific venous hemoglobin concentrations. There are significant changes in the positions of some points, such as that marked by a 1. This point, which was found to be CIN 2 by hospital pathology but not by the study pathologist, is now nearer the site which was found to be CIN 2 in both histopathology evaluations (the brown square).

5 Discussion

5.1 *Comparison to Previous Reports of Pressure Dependent Hemoglobin Parameters*

The effects of pressure on the determination of hemoglobin concentrations have been previously investigated. In a mouse thigh muscle model oxygenation and blood vessel radius both decreased as pressure increased from 0 to 200 $\mathrm{mN/mm^2}$, while blood volume fraction was nearly constant.[17] These results are nearly perfectly contradictory to ours in which blood vessel radius and oxygenation did not show a dependence on pressure, but hemoglobin concentration decreased. Therefore, we compare the differences in the two experiments and analysis methods.

Reif et al.[17] used the correction factor of Svaasand et al.[11] to correct for the fact that hemoglobin is in blood vessels. Although the difference in correction factors will result in a difference in results, the general correlations we found in Fig. 6 indicate that it should not effect trends. In both the analysis methods, the pathlength was assumed to decrease with increasing absorption. However, the model used was slightly different. Reif et al. assumed $L = b/(\mu_a \mu_s')^c$, where b and c were determined in the previous work to be 0.22 and 0.20, respectively, for the specific probe used and the reduced scattering coefficient, μ_s' had the form $d(\lambda^{-e})$, where d and e were fit parameters. This is in contrast to our work in which the effective pathlength decrease is modeled by a ninth-order polynomial function of μ_a that was determined using a small range of scattering parameters for the specific probe used. The different parameterization of the pathlength dependence on μ_a could be a source of the difference in results. Our effective pathlength shown in Fig. 4(c) could not be fit using a power law function of μ_a such as Reif et al. used.

Reif et al. fit a much larger spectral range and consequently accurate modeling of the diffuse reflectance, $I(0)$, was much more important. The parameterization of $I(0)$ was very similar to that used here [Eq. (10)], except that there was no additive constant. Also, the wavelength range included the strong Soret absorption bands of hemoglobin, consequently accurate correction of μ_a was needed over a wider range of absorption values. Finally, we note that Reif et al. measured mouse thigh muscle whereas we measured human cervical epithelium. The two tissues may have different hemodynamic responses to pressure. Evidence for differences in hemodynamic responses to pressure is discussed below.

The effects of pressure on the measurement of hemoglobin parameters in the mucosal lower lip have been investigated.[24] Two pressures were used; gentle (9 to 12 $\mathrm{mN/mm^2}$) and firm 150 to 200 $\mathrm{mN/mm^2}$. For tissue interrogation depths similar to that used in this study, the total hemoglobin concentration measured was less for the firm than the gentle pressure. The hemoglobin packaging length scale (proportional to vessel diameter) also decreased slightly with the firmer pressure. These results, using a tissue with similarities to cervical epithelium, but a wider range of pressures, are similar to ours.

Pressure also has an effect on the hemoglobin parameters determined from optical measurements of skin.[18] Lim et al. used a fiber optic probe similar to the one used in this study,

except that the source–detector separation was 350 μm (instead of 550 μm) and the numerical aperture of the fibers was 0.22 (instead of 0.37). They measured skin of the neck, finger, and forehead. The measured concentration of hemoglobin decreased with pressure and time for all skin sites measured. Oxygen saturation also decreased with time when the pressure was >22 mN/mm^2. The hemoglobin packing factor had very little dependence on pressure (or time) for the neck and forehead, but decreased with time when the pressure was applied in measurements of fingers. The authors concluded that probe pressure effects depend on the anatomical site.

A study on the effects of pressure on determination of hemoglobin parameters from the cervix found that hemoglobin concentration but not oxygenation was affected by probe pressure, consistent with our results.[25] Interesting, the model used did not account for the fact that blood is confined to blood vessels, but did take into account the two layer nature of cervical epithelium.

5.2 *Mitigating the Effects of Pressure*

To avoid probe pressure effects, noncontact reflectance measurement systems have been proposed,[26] and in some cases demonstrated.[27–29] Vessel diameter has only been reported for one of these systems and details of how pathlength was handled in the data fitting procedure were not provided.[27] Accurate determination of vessel diameter and density with these systems will require an understanding of how the light travels through the tissue and how the distance traveled through hemoglobin containing tissue depends on the blood vessel size and density. A possible draw back to these noncontact systems is that the lenses used in initial designs are too large to make them practical for endoscopy or in other spatially constrained regions.

5.3 *Challenges to Accurate Determination of Vasculature Characteristics*

Extraction of accurate hemoglobin parameters from tissue is difficult not only because the placement of fiber optic probes may compress the tissue but also because the tissue is heterogeneous. The heterogeneity of tissue has multiple aspects. One is that the hemoglobin is in blood vessels of varying sizes. Here, as in past work,[11–15] the assumption was made that all blood vessels in the sampled tissue are the same size. Another aspect of tissue heterogeneity is that epithelial tissues are layered. The thickness of the top cellular layer can vary from patient-to-patient and within a patient. For example, immature (metaplastic) squamous epithelium is thinner than mature squamous epithelium. Similarly, the columnar epithelium of the cervix will have a different thickness than the squamous epithelium. In this work, we assumed only one thickness for the cellular epithelium. Potentially, different measurement geometries could be used to provide information about the epithelial thickness. Another approximation made in this work when determining the effects of absorption on the effective pathlength was that the scattering properties were the same in the cellular epithelium and in the stroma. Others have assumed different scattering properties for the stroma and the cellular layer.[30] Nonetheless, because the light does not penetrate deeply into the stroma and because the scattering parameters are not known precisely for either layer and may vary from site to site, we chose to determine an average effective pathlength obtained from Monte Carlo simulations using several sets of scattering parameters.

The determined vessel size and tissue hemoglobin concentration depend on the value of blood hemoglobin used in the fits. We tried determining blood hemoglobin concentration from the data fits, but found that when blood hemoglobin was a fit parameter, the errors of the returned fit parameters were as large as their values. Venous blood hemoglobin values provide a patient specific value, however, the blood hemoglobin concentration in the cervical stroma may be different. The hematocrit of the capillaries is less than the venous hematocrit due to the Fåhraeus effect, a dilution of red blood cells because of the difference in flow speeds of plasma and red-blood-cells in the capillaries. The difference in venous and capillary hemoglobin concentration tends to be greater when the hemoglobin concentrations are lower.[31]

6 Conclusions

A physically based derivation of a correction factor to the absorption coefficient due to hemoglobin being present only in blood vessels shows that this correction depends both on the size of the blood vessels and on the concentration of blood vessels. Previous derivations did not account for the dependence of the correction factor on the density of blood vessels. Comparison of data fits using our correction factor and a commonly used previously derived correction factor showed differences that are significant compared to the measured values and consequently would be important to any diagnostic using this information.

Determination of hemoglobin concentration in *in vivo* cervical tissue depends on the applied probe pressure as shown both by our measurements and Chang et al.[25] Our results indicate that vessel density but neither vessel size nor oxygenation depend on the probe pressure. Comparison of our results with measurements made on different tissues demonstrates that probe pressure effects are likely tissue dependent.

Four parameters are obtained from our analysis of *in vivo* cervical epithelial data, effective vessel radius, effective vessel density, hemoglobin oxygenation, and average tissue hemoglobin concentration. The one site in our data set that was found to be CIN 2/3 by both hospital and study pathologist evaluation was at the edge of the data in plots of hemoglobin parameters indicating that these parameters may be useful.

Several challenges remain for the accurate measurement of vasculature parameters via diffuse reflectance and for the demonstration that this information is useful for tissue diagnostics. Although our determination of hemoglobin parameters takes into account the dependence of the effective pathlength on absorption, several approximations were made which could reduce the accuracy of the results. Both vessel diameter and hemoglobin concentration depend on the value used for blood hemoglobin concentration. Obtaining the accurate values for blood hemoglobin is difficult because a venous blood draw is necessary, and assumptions must be made about how the cervical epithelial capillary hemoglobin concentration is related to venous hemoglobin concentration. The effects of probe pressure must also be mitigated either by noncontact measurements[27] or by rapid measurement upon detection of probe-tissue contact.[32]

Acknowledgments

This work was funded by NIH CA71898.

References

1. M. Raica, A. M. Cimpeana, and D. Ribatti, "Angiogenesis in pre-malignant conditions," *Eur. J. Cancer* **45**(11), 1924–1934 (2009).
2. A. K. Tiwari et al., "Neo-angiogenesis and the premalignant micro-circulatory augmentation of early colon carcinogenesis," *Cancer Lett.* **306** (2), 205–213 (2011).
3. H. H. Oliveira-Neto et al., "A comparative study of microvessel density in squamous cell carcinoma of the oral cavity and lip," *Oral Surg. Oral Med. Oral Pathol. Oral Radiol.* **113**(3), 391–398 (2012).
4. M. Astekar et al., "Expression of vascular endothelial growth factor and microvessel density in oral tumorigenesis," *J. Oral Maxillofac. Pathol.* **16**(1), 22–26 (2012).
5. W. W. L. Choi et al., "Angiogenic and lymphangiogenic microvessel density in breast carcinoma: correlation with clinicopathologic parameters and VEGF-family gene expression," *Mod. Pathol.* **18**, 143–152 (2005).
6. V. T.-C. Chang et al., "Visible light optical spectroscopy is sensitive to neovascularization in the dysplastic cervix," *J. Biomed. Opt.* **15**(5), 057006 (2010).
7. S. P. Dobbs et al., "Angiogenesis is associated with vascular endothelial growth factor expression in cervical intraepithelial neoplasia," *Br. J. Cancer* **76**(11), 1410–1415 (1997).
8. K. K. Smith-McCune and N. Weidner, "Demonstration and characterization of the angiogenic properties of cervical dysplasia," *Cancer Res.* **54**(3), 800–804 (1994).
9. A. Obermair et al., "Correlation of vascular endothelial growth factor expression and microvessel density in cervical intraepithelial neoplasia," *J. Natl. Cancer Inst.* **89**(16), 1212–1217 (1997).
10. S. Fantini and A. Sassaroli, "Near-infrared optical mammography for breast cancer detection with intrinsic contrast," *Ann. Biomed. Eng.* **40**(2), 398–407 (2012).
11. L. O. Svaasand et al., "Therapeutic response during pulsed laser treatment of port-wine stains: dependence on vessel diameter and depth in dermis," *Lasers Med. Sci.* **10**, 235–243 (1995).
12. H. Liu et al., "Influence of blood vessels on the measurement of hemoglobin oxygenation as determined by time-resolved reflectance spectroscopy," *Med. Phys.* **22**(8), 1209–1217 (1995).
13. A. Talsma, B. Chance, and R. Graaff, "Corrections for inhomogeneities in biological tissue caused by blood vessels," *J. Opt. Soc. Am. A* **18**(4), 932–939 (2001).
14. W. Verkruysse et al., "Modelling light distributions of homogeneous versus discrete absorbers in light irradiated turbid media," *Phys. Med. Biol.* **42**(1), 51–65 (1997).
15. R. L. P. van Veen, W. Verkruysse, and H. J. C. M. Sterenborg, "Diffuse-reflectance spectroscopy from 500 to 1060 nm by correction for inhomogeneously distributed absorbers," *Opt. Lett.* **27**(4), 246–248 (2002).
16. C. Lau et al., "Re-evaluation of model-based light-scattering spectroscopy for tissue spectroscopy," *J. Biomed. Opt.* **14**(2), 024031 (2009).
17. R. Reif et al., "Analysis of changes in reflectance measurements on biological tissues subjected to different probe pressures," *J. Biomed. Opt.* **13**(1), 010502 (2008).
18. L. Lim et al., "Probe pressure effects on human skin diffuse reflectance and fluorescence spectroscopy measurements," *J. Biomed. Opt.* **16**(1), 011012 (2011).
19. A. Amelink and H. J. C. M. Sterenborg, "*In vivo* measurement of the local optical properties of tissue by use of differential path-length spectroscopy," *Opt. Lett.* **29**(10), 1087–1089 (2004).
20. J. R. Mourant et al., "*In vivo* light scattering for the detection of cancerous and precancerous lesions of the cervix," *Appl. Opt.* **48**(10), D26–D35 (2009).
21. Scott Prahl Oregon Medical Laser Center, http://omlc.ogi.edu/spectra/hemoglobin/ (1999).
22. J. W. Sellors and R. Sankaranarayanan, *Colposcopy and Treatment of Cervical Intraepithelial Neoplasia. A Beginners Manual International Agency for Research on Cancer*, IARC Press, Lyon Cedex, France (2003).
23. R. A. Freitas, *Nanomedicine, Vol. I: Basic Capabilities*, p. 213, Landes Bioscience, Austin, TX (1999).
24. S. Ruderman et al., "Analysis of pressure, angle and temporal effects on tissue optical properties from polarization-gated spectroscopic probe measurements," *Biomed. Opt. Express* **1**(2), 489–499 (2010).
25. V. T.-C. Chang et al., "Towards a field-compatible optical spectroscopic device for cervical cancer screening in resource-limited settings: effects of calibration and pressure," *Opt. Express* **19**(19), 117908–117925 (2011).
26. C. Zhu and Q. Liu, "Numerical investigation of lens based setup for depth sensitive diffuse reflectance measurements in an epithelial cancer model," *Opt. Express* **20**(28), 29807–29822 (2012).
27. S. F. Bish et al., "Development of a noncontact diffuse optical spectroscopy probe for measuring tissue optical properties," *J. Biomed. Opt.* **16**(12), 120505 (2011).
28. S. Andree and C. Reble, "Evaluation of a novel noncontact spectrally and spatially resolved reflectance setup with continuously variabsource-detector separation using silicone phantoms," *J. Biomed. Opt.* **15**(6), 067009 (2010).
29. N. Bedard et al., "Multimodal snapshot spectral imaging for oral cancer diagnostics: a pilot study," *Biomed. Opt. Express* **4**(6), 938–949 (2013).
30. D. Arifler et al., "Spatially resolved reflectance spectroscopy for diagnosis of cervical precancer: Monte Carlo modeling and comparison to clinical measurements," *J. Biomed. Opt.* **11**(6), 064027 (2006).
31. W. G. Murphy, E. Tong, and C. Murphy, "Why do women have similar erythropoietin levels to men but lower hemoglobin levels?" *Blood* **116**(15), 2861–2862 (2010).
32. S. Ruderman et al., "Method of detecting tissue contact for fiber-optic probes to automate data acquisition without hardware modification," *Biomed. Opt. Express* **4**(8), 1401–1412 (2013).

Biographies of the authors are not available.